tvst

Glaucoma

MiR-29b Downregulation by p53/Sp1 Complex Plays a Critical Role in Bleb Scar Formation After Glaucoma Filtration Surgery

Ning Li[1,*], Zixi Wang[2,*], Fan Yang[1], Wenjun Hu[3], Xiaojun Zha[2], and Xuanchu Duan[4–6]

[1] Department of Ophthalmology, The First Affiliated Hospital of Anhui Medical University, Hefei, China
[2] Department of Biochemistry and Molecular Biology, School of Basic Medicine, Anhui Medical University, Hefei, China
[3] Department of Clinical Laboratory, The First Affiliated Hospital of Anhui Medical University, Hefei, China
[4] Medical School of Ophthalmology and Otorhinolaryngology, Hubei University of Science and Technology, Xianning, China
[5] Aier School of Ophthalmology, Central South University, Changsha, China
[6] Changsha Aier Eye Hospital, Aier Eye Hospital Group, Changsha, China

Correspondence: Xiaojun Zha, Department of Biochemistry and Molecular Biology, School of Basic Medicine, Anhui Medical University, Hefei 230033, China. e-mail: zhaxiaojunpumc@gmail.com
Xuanchu Duan, Aier School of Ophthalmology, Central South University, Changsha 410000, China. e-mail: duanxchu@csu.edu.cn

Received: March 4, 2023
Accepted: September 24, 2023
Published: December 5, 2023

Keywords: bleb scarring; fibroblasts; glaucoma filtration surgery; miR-29b; specificity protein 1; tumor protein p53

Citation: Li N, Wang Z, Yang F, Hu W, Zha X, Duan X. MiR-29b downregulation by p53/Sp1 complex plays a critical role in bleb scar formation after glaucoma filtration surgery. Transl Vis Sci Technol. 2023;12(12):5, https://doi.org/10.1167/tvst.12.12.5

Purpose: To investigate the function and mechanism of tumor protein p53 in pathological scarring after glaucoma filtration surgery (GFS) using human Tenon's fibroblasts (HTFs) and a rabbit GFS model.

Methods: The expression of p53 in bleb scarring after GFS and transforming growth factor-β (TGF-β)–induced HTFs (myofibroblasts [MFs]) was examined by western blot and immunochemical analysis. The interaction between p53 and specificity protein 1 (Sp1) was investigated by immunoprecipitation. The role of p53 and Sp1 in the accumulation of collagen type I alpha 1 chain (COL1A1) and the migration of MFs was evaluated by western blot, quantitative real-time polymerase chain reaction (qRT-PCR), wound healing, and Transwell assay. The regulatory mechanisms among p53/Sp1 and miR-29b were detected via qRT-PCR, western blot, luciferase reporter assay, and chromatin immunoprecipitation assay. The therapeutic effect of mithramycin A, a specific inhibitor of Sp1, on scarring formation was evaluated in a rabbit GFS model.

Results: p53 was upregulated in bleb scar tissue and MFs. p53 and Sp1 form a transcription factor complex that induces the accumulation of COL1A1 and promotes the migration of MFs through downregulation of miR-29b, a known suppressor of COL1A1. The p53/Sp1 axis inhibits miR-29b expression by the direct binding promoter of the miR-29b gene. Mithramycin A treatment attenuated bleb scar formation in vivo.

Conclusions: The p53/Sp1/miR-29b signaling pathway plays a critical role in bleb scar formation after GFS. This pathway could be targeted for therapeutic intervention of pathological scarring after GFS.

Translational Relevance: Our research indicates that inhibition of p53/Sp1/miR-29b is a promising therapeutic strategy for preventing post-GFS pathological scarring.

Introduction

The incidence of glaucoma, one of the leading causes of irreversible blindness worldwide, has gradually increased in recent years,[1] with more than 100 million patients expected by 2040.[2] Glaucoma filtration surgery (GFS) is widely used as an effective treatment for glaucoma, but it has a failure rate at 1 year of 15%.[3] After GFS, human Tenon's fibroblasts (HTFs) proliferate and differentiate into myofibroblasts (MFs), which increases collagen deposition and causes filtration tract, or bleb, scarring. This phenomenon can be triggered by many factors, such as operative intervention, pre-existing conditions, genetics, and state of aqueous and hydraulic stress (aqueous passage

through tissue).[4–6] A key factor for the long-term success of GFS is the prevention of scar formation by inhibiting the overactivation of HTFs and subsequent accumulation of collagen. Previous studies have indicated that some molecular compounds, such as AR12286, can alleviate transforming growth factor-β (TGF-β)–related MF transdifferentiation and reduce fibrosis after GFS.[7] However, the molecular mechanisms underlying pathological scarring in GFS remain unclear.

MicroRNAs (miRNAs) are a class of non-coding RNAs with a length of 17 to 25 nucleotides that typically bind to specific mRNA to mediate their molecular function.[8] In recent years, the role of miRNA in various diseases, particularly with regard to tumor diagnosis, treatment, prognosis, and recurrence, has been investigated.[9–11] In particular, miR-26a has been reported to be involved in scar formation after GFS.[12] Previously, we conducted a study to determine the role of miR-29b after GFS. We found that miR-29b could suppress type I collagen expression via the phosphoinositide 3-kinase (PI3K)/protein kinase B (Akt) pathway in HFTs.[13] Thus, miRNAs may synergistically regulate individual genes for important biological processes, such as scar formation after GFS.

Tumor protein p53, an important tumor suppressor, is abnormally expressed in various tumors.[14,15] In addition, p53 plays a vital role in organ fibrosis, such as liver, renal, and cardiac fibrosis.[16–18] For example, increased expression of the p53/miR-34 feedback loop leads to apoptosis in alveolar epithelial cells, contributing to the pathogenesis of pulmonary fibrosis via fibroblast proliferation.[19] However, the role of p53 in bleb scarring after GFS remains unclear.

Materials and Methods

Sample Collection and Masson's Trichrome Staining

In compliance with the tenets of the Declaration of Helsinki, the pathological tissue was derived from scar tissue collected from filtering channels of patients with uncontrolled intraocular pressure (IOP) after GFS. Normal control tissues were obtained from excised Tenon's capsule specimens during strabismus surgery.[20] The tissue samples were collected with the written consent of the patients before surgery. Tissue samples were fixed overnight in 10% formalin, cut into 5-µm sections, and stained with Masson's trichrome according to the manufacturer's instructions for histological examination. To assess the collagen volume fraction (CVF = collagen area/total area), eight separate views (400× magnification) were selected.

Immunohistochemistry Staining

Scar and control tissues obtained during GFS were collected and fixed in 4% paraformaldehyde solution. The slides were embedded in paraffin and cut into 4-µm sections. The sections were then blocked with 5% goat serum, and primary antibodies were added according to the manufacturer's instructions. Sections were incubated with diluted p53 (1:200) and visualized with a horseradish peroxidase–conjugated secondary antibody and 3,3′-diaminobenzidine (DAB). Results were obtained under a random field of view at 400× magnification.

Real-Time Polymerase Chain Reaction

The total RNA was extracted from the cells and tissue samples using TRIzol Reagent (Genesand, Beijing, China). We used an M-MLV Reverse Transcriptase kit (TransGen Biotech, Beijing, China) to synthesize cDNA, and real-time polymerase chain reaction (RT-PCR) was performed using SYBR Premix Ex Taq II (Takara Bio, Shiga, Japan) in a PCR system (Applied Biosystems, Waltham, MA), according to the manufacturer's protocol. The expression of miR-29b was detected using the Hairpin-it miRNA qPCR Quantitation Kit (GenePharma, Shanghai, China), according to the manufacturer's instructions. The relative expression levels of the target genes were normalized using glyceraldehyde 3-phosphate dehydrogenase (GAPDH) or RNA (U6 small nuclear 1) and calculated using the $2^{-\Delta\Delta Ct}$ formula. The primer sequences were as follows: GAPDH—forward 5′-GAAGGTCGGAGTCAACGGATTT-3′, reverse 5′-CCTGGAAGATGGTGATGGGATT-3′; miR-29b (human)—forward 5′-TCAGGAAGCTGGTTTCATATGGT-3′, reverse 5′-CCCCCAAGAACACTGATTTCAA-3′; Sp1—forward 5′-TCACTCCATGGATGAAATGACA-3′, reverse 5′-CAGAGGAGGAAGAGATGATCTG-3′; p53—forward 5′-TTCCTGAAAACAACGTTCTGTC-3′, reverse 5′-AACCATTGTTCAATATCGTCCG-3′; COL1A1—forward 5′-AAAGATGGACTCAACGGTCTC-3′, reverse 5′-CATCGTGAGCCTTCTCTTGAG-3′; U6 (human)—forward 5′-CAGCACATATACTAAAATTGGAACG-3′, reverse: 5′-ACGAATTTGCGTGTCATCC-3′; miR-29b (rabbit)—forward 5′- ATCGTGCGTAGCACCATTTGAAAT-3′, reverse 5′-ATCCAGTGCAGGGTCC

GAGG-3′; and U6 (rabbit)—forward 5′- AGCAGCG GTTCGGAGGATG-3′, reverse:5′- TTCGGGTACT GGGAATCTCTCAC-3′.

Western Blot

Western blot was performed as previously described.[21] Radioimmunoprecipitation assay (RIPA) buffer (Beyotime Biotechnology, Jiangsu, China) was used for cellular protein extraction. The proteins were then separated by electrophoresis and transferred to polyvinylidene fluoride (PVDF) membranes (Merck Millipore, Burlington, MA). After blocking with 5% skim milk for 1 hour, the primary antibody solution was incubated at 4°C overnight. Finally, the cells were incubated with horseradish peroxidase–conjugated secondary antibody solution for 1 hour and detected using chemiluminescence (Thermo Fisher Scientific, Waltham, MA). Monoclonal antibodies against Sp1, p53, and COL1A1 were obtained from Cell Signaling Technology (Danvers, MA). GAPDH (Abcam, Cambridge, UK) was used as a loading control.

Cell Culture and Drug Treatment

Human subconjunctival fibroblasts (HTFs) were obtained as described previously.[13] HTFs (passages 3–6) were cultured to 80% to 85% confluence prior to passaging and were treated with or without 10 ng/mL TGF-β1 (PeproTech, Cranbury, NJ) in serum-free medium for 48 hours as MFs. HEK-293T cells (ATCC, Manassas, VA) were cultured in Dulbecco's Modified Eagle Medium (DMEM; Boster Bio, Pleasanton, CA) supplemented with 10% fetal calf serum, 1% L-glutamine (2 mM), 50 g/mL penicillin, and streptomycin at 37°C in 5% CO_2. Mithramycin A (MedChemExpress, Shanghai, China) was dissolved in dimethyl sulfoxide (DMSO; Sigma-Aldrich, St. Louis, MO) and diluted to working concentrations of 0, 50, 100, and 200 nM.

Transient Transfection

Short interfering RNAs (siRNAs) for p53 and Sp1 were purchased from Thermo Fisher Scientific. The sequences were as follows: Sp1—5′-CCAUUAACCUCAGUGCAUUTT-3′; p53—5′-CGGCGCACAGAGGAAGAGAAUCUC-3′; miR-29b mimics—5′-UAGCACCAUUUGAAAUCAGUGUU-3′; and mimics negative control (NC)—5′-UUCUCCGAACGUGUCACGUTT-3′. Well-conditioned cells were seeded into 12-well plates and transfected with siRNA using Lipofectamine RNAiMax (GenePharma, Shanghai, China).

Vectors and Infections

All of the lentiviruses were purchased from GenePharma. The p53 or Sp1 overexpressing cell lines were constructed using empty lentiviruses and viruses expressing full-length sequences of them. HTFs were instantly infected with lentiviral particles in the presence of 10 μg/mL Polybrene (GenePharma). Puromycin (MedChemExpress) was also used to screen for 1 week. The transfected cells were collected for subsequent experiments.

Transwell Assays

The cells (20,000 cells per well) were inoculated into the upper chamber of the Transwell (12 μm; Corning Inc., Corning, NY) The upper chamber contained serum-free medium, and the bottom chamber contained complete medium. After 48 hours, the cells were washed with phosphate-buffered saline (PBS) and stained with crystal violet after fixation with paraformaldehyde. Images of the stained cells were captured, and cells were counted from five random fields using an optical microscope (Leica DM6B; Leica Microsystems, Wetzlar, Germany) for each sample in triplicate.

Wound Healing Assays

Well-conditioned cells were seeded in 24-well plates. When the cells grew to approximately 80% confluency, a 10-μL pipette tip was used to slowly scrape the cell monolayer in a straight line at the center of each well. The cells were rinsed with PBS to remove cellular debris and subsequently incubated at 37°C for 24 hours. Images were acquired using a light microscope (Leica DM6 B). The scratched area was visualized and quantified using ImageJ (National Institutes of Health, Bethesda, MD).

Immunoprecipitation

Immunoprecipitation was performed using an immunoprecipitation system kit (Merck Millipore), and experiments were performed according to the manufacturer's instructions. Briefly, 2 mg of cellular protein lysate was mixed with anti-p53 or immunoglobulin G (IgG) and 10 μL of the affinity ligand for immunoprecipitation. Proteins were eluted from the washed immune complexes and blotted with the appropriate antibodies.

Luciferase Reporter Gene Assay

The luciferase reporter gene assay was performed as previously described.[22] Briefly, a 243-bp fragment of the miR-29b promoter (−1141/−1383) containing the Sp1 binding site was obtained by PCR using genomic DNA. The primer sequences were as follows: forward 5′-AAATACAA GCCAAGGGAACAGACTAAGT-3′, reverse 5′-TACCCACAAATATCCAGCCTACATCC-3′. The fragment was cloned into the BglII and KpnI sites of the pGL3 promoter plasmid miR-29b-Luc. A Q5 Site-Directed Mutagenesis Kit (New England Biolabs, Ipswich, MA) was used to mutate the potential Sp1 binding site (miR-29b-Luc-mut). The primer sequences were as follows: forward 5′- AAAAGG TTGGCATGTGTTTTGAGGCTAAAAG-3′, reverse 5′- CTTTGGCTTGTTTTATCATG-3′. HEK-293T cells were seeded in 24-well plates overnight and subsequently transfected with reporter vectors for miR-29b-Luc (100 ng) or miR-29b-Luc-mut, *Renilla* luciferase (50 ng), and the Sp1 expression vector pcDNA3.1-Sp1 or the empty vector pcDNA3.1 (100 ng) as control (GenePharma) The cells were collected, and firefly and *Renilla* luciferase activities were measured using a Dual-Luciferase Reporter Assay System (Promega, Madison, WI), according to the manufacturer's instructions. Firefly and *Renilla* luciferase activities were measured. Relative luciferase activity was calculated as the ratio of firefly luciferase activity to *Renilla* luciferase activity.

Chromatin Immunoprecipitation

Chromatin immunoprecipitation (ChIP) assays were performed using EZ-ChIP assay kits (EMD Millipore, Burlington, MA), according to the manufacturer's protocols. Antibodies against Sp1 were purchased from Abcam. The primer sequences were as follows: putative Sp1 binding site region of human miR-29b (PBR)—forward 5-GGATTGGAGCCTGGTTTTCACA-3′, reverse 5′-GCCTACATCCAACTTCTCCCACTTTC-3.

Glaucoma Filtration Surgery in Rabbits

The rabbit model of chronic ocular hypertension was constructed as previously described using 2-year-old adult male rabbits (*Oryctolagus cuniculus*) weighing 2.5 to 3.5 kg.[23] Subconjunctival injection with different concentrations of mithramycin A was administered beside the filtering bleb using a sterile microinjector on postoperative days 3 and 10. We harvested the ocular tissues, including conjunctiva, Tenon's capsule, and sclera, from the bleb area on D28 after performing trabeculectomy. All animals were maintained in strict accordance with the guidelines of the Animal Center of Anhui Medical University, and all animal experimental procedures were approved by the Experimental Animal Ethics Committee of Anhui Medical University (20211302).

Statistical Analysis

All values are expressed as mean ± SD. Comparisons between two groups were performed using an unpaired Student's *t*-test (Prism; GraphPad, San Diego, CA). Statistical significance was set at $P < 0.05$.

Results

Increased p53 Expression in Scarring After Filtration Surgery

To investigate the role of p53 during scar formation, p53 expression was examined in both normal Tenon's tissues (control tissues) and scar tissues from patients following GFS. Masson's trichrome and immunohistochemical staining demonstrated a higher level of p53 in the scar tissue as compared to the control tissues (Fig. 1A). Similarly, the mRNA and protein expression levels of p53 and COL1A1 were clearly higher in the scar tissues than in the control tissues (Figs. 1B, 1C). These results suggest that p53 is upregulated in scar tissues following GFS.

p53 Promotes COL1A1 Expression and Cell Migration of HTFs and MFs

To further investigate the role of p53 in scarring following GFS, we isolated primary HTFs and transformed them into MFs through treatment with TGF-β in vitro. Consistent with the clinical results, whether regarding protein or mRNA levels, the expression of p53 was substantially greater in MFs than in HTFs (Figs. 2A, 2B). Then, we constructed p53-overexpressing HTFs using lentivirus and p53 knockdown MFs using siRNA. The results showed that increased p53 expression promoted COL1A1 expression in HTFs (Figs. 2C, 2D), whereas decreased p53 expression suppressed COL1A1 expression in MFs (Figs. 2E, 2F). Furthermore, the results of wound healing and Transwell assay showed that p53 overexpression increased the migration of HTFs (Figs. 2G, 2H), whereas p53 knockdown decreased the migration of MFs (Figs. 2I, 2J). Thus, these results suggest

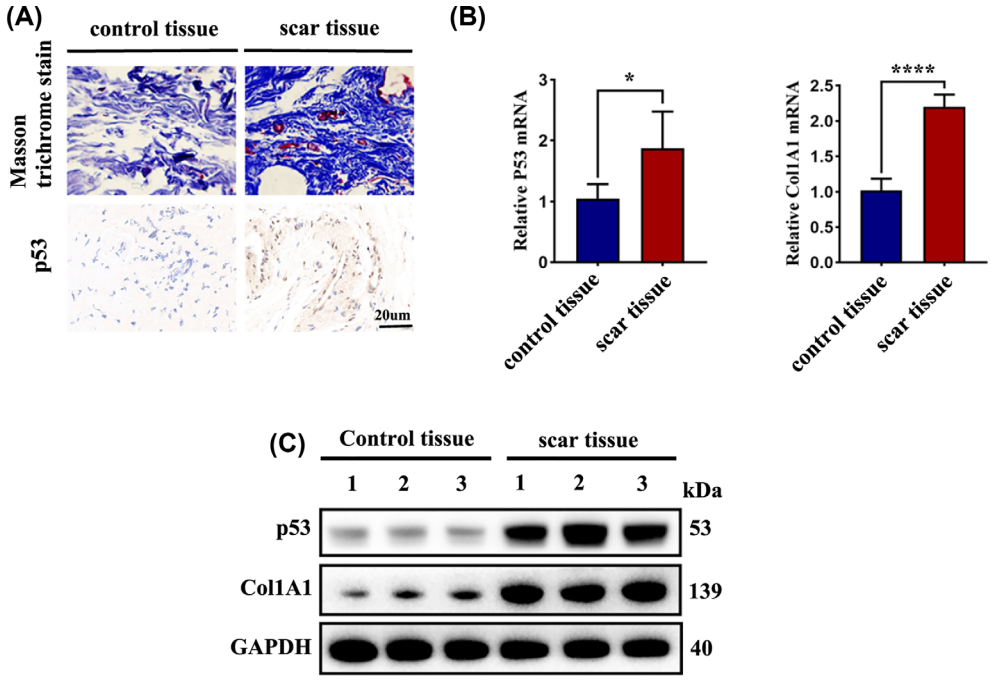

Figure 1. Increased p53 expression in bleb scar tissue after filtration surgery. (**A**) Masson's trichrome and immunohistochemical staining of human Tenon's capsule specimens and scar tissue from GFS patients. (**B**, **C**) The levels of p53 and COL1A1 in the indicated tissues were detected by quantitative PCR (qPCR) (**B**) and western blotting (**C**). Data with *error bars* represent mean ± SD. *$P < 0.05$, ****$P < 0.0001$.

that p53 promotes the accumulation of COL1A1 and the migration ability in HTFs and MFs.

p53 Mediates COL1A1 Expression and Cell Migration Via Sp1

Next, we investigated the mechanism underlying the promotion of COL1A1 expression by p53 in HTFs. Previous studies have found that Sp1 regulates the expression of COL1A1 and that p53 interacts with Sp1 to activate downstream signaling.[24–26] Therefore, we hypothesized that p53 mediates COL1A1 expression via direct interaction with Sp1. We confirmed that p53 bound to Sp1 in MFs (Fig. 3A), and, in subsequent experiments, we found that Sp1 plays a role similar to that of p53 in HTFs. When we overexpressed Sp1 in HTFs, there was a substantial increase in COL1A1 expression (Figs. 3B, 3C) and the migration of HTFs (Figs. 3D, 3E). Conversely, Sp1 knockdown by siRNA resulted in COL1A1 downregulation and decreased MFs migration (Figs. 3F, 3G, 3L, 3M). Administration of mithramycin A, an inhibitor that can selectively inhibit transcriptional activity of Sp1,[27,28] inhibited the expression of COL1A1 in MFs in a dose-dependent manner (Figs. 3F, 3J, 3K) and substantially reduced MF migration (Figs. 3L, 3M). Therefore, the migration of HTFs and MFs was induced by Sp1.

To further determine whether Sp1 is involved in upregulated expression of COL1A1 mediated by p53, we used Sp1 siRNAs to knock down Sp1 in p53 overexpressing HTFs. As shown in Figures 4A to 4D, depletion of Sp1 led to a substantial decrease in COL1A1expression and the migration of HTFs. Moreover, treatment of p53 overexpressing HTFs with mithramycin A resulted in a similar result (Figs. 4E–4H). Taken together, these results suggest that p53 promotes the expression of COL1A1 and cell migration via Sp1.

Sp1 Inhibits the Expression of miR-29b Through Binding With Its Promoter

Next, we investigated the mechanism by which the p53/Sp1 axis promotes COL1A1 expression. In a previous study, we found that miR-29b acts as a suppressor of COL1A1 HTFs.[13] Therefore, we hypothesized that the activation of p53/Sp1 signaling may promote COL1A1 expression via the inhibition of miR-29b transcription in HTFs. As shown in Figure 5A, overexpression of either p53 or Sp1 led to downregulated expression of miR-29b, whereas simultaneous expression of p53 and Sp1 dramatically inhibited miR-29b expression. In contrast, the knockdown of p53 and/or Sp1 yielded the opposite result

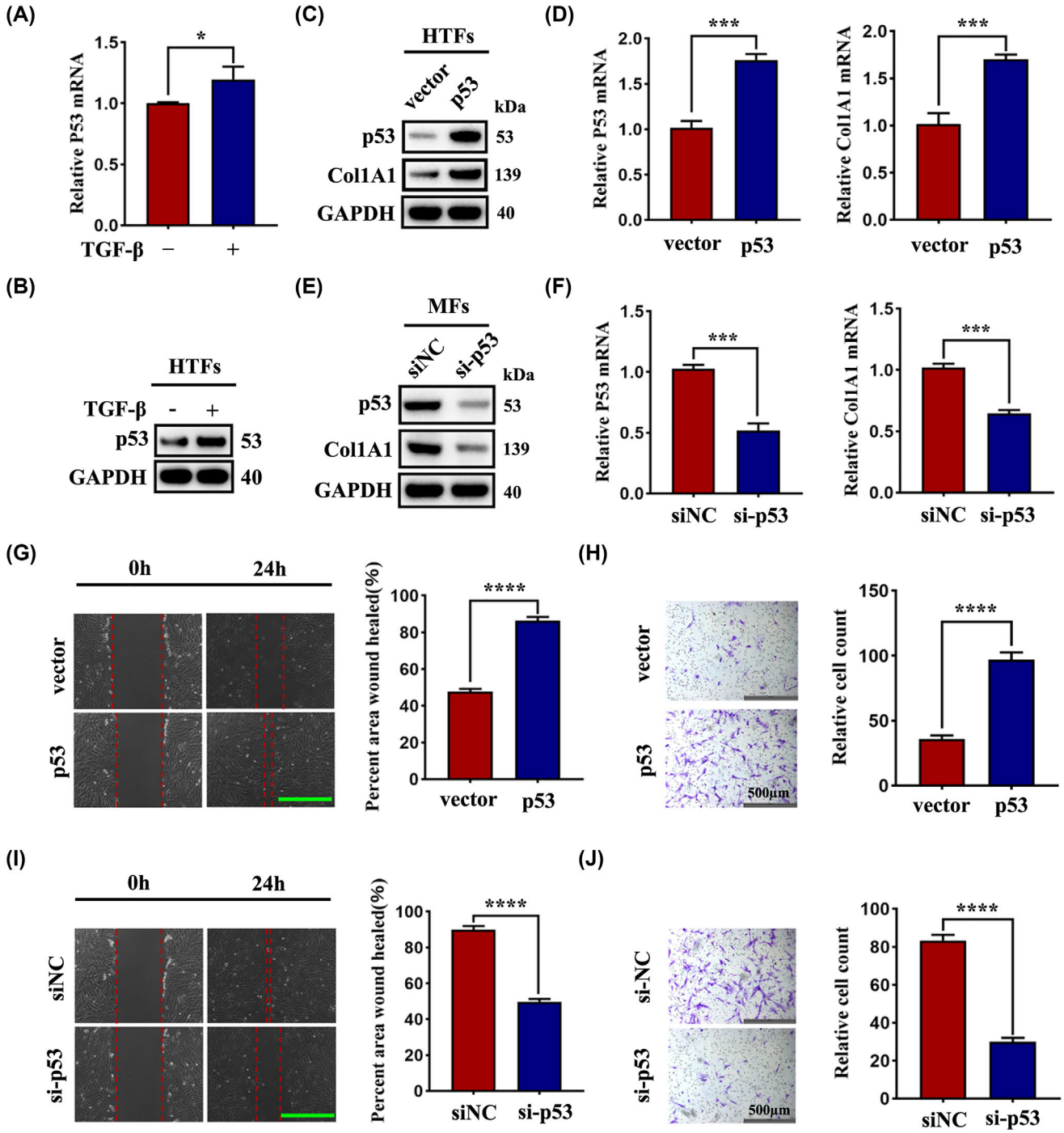

Figure 2. The activation of p53 promotes COL1A1 expression and cell migration in HTFs and MFs. (**A**, **B**) HTFs were treated with 10 ng/mL TGF-β1 for 48 hours. The level of p53 was detected by using qPCR (**A**) and western blotting (**B**). (**C**–**J**) HTFs were infected with lentiviruses expressing either p53 or empty control vector; MFs were transduced with p53 siRNA or siRNA negative control (siNC). p53 and COL1A1 expression of the indicated cells was evaluated by western blotting (**C**, **E**) and qPCR (**D**, **F**). Wound healing (**G**, **I**) and Transwell assays (**H**, **J**) were used to measure the migration ability of the indicated cells. Representative images (*left panel*) and statistical analysis (*right panel*) are shown. Data with *error bars* represent mean ± SD. *$P < 0.05$, ***$P < 0.001$, ****$P < 0.0001$.

(Fig. 5B). Moreover, administration of mithramycin A led to upregulation of miR-29b in a dose-dependent manner in HTFs (Fig. 5C). Strikingly, ectopic expression of miR-29b attenuated the upregulated COL1A1 induced by p53 or Sp1 overexpression (Figs. 5D, 5E), suggesting that miR-29b is likely involved in the regulation of COL1A1 by the p53/Sp1 axis.

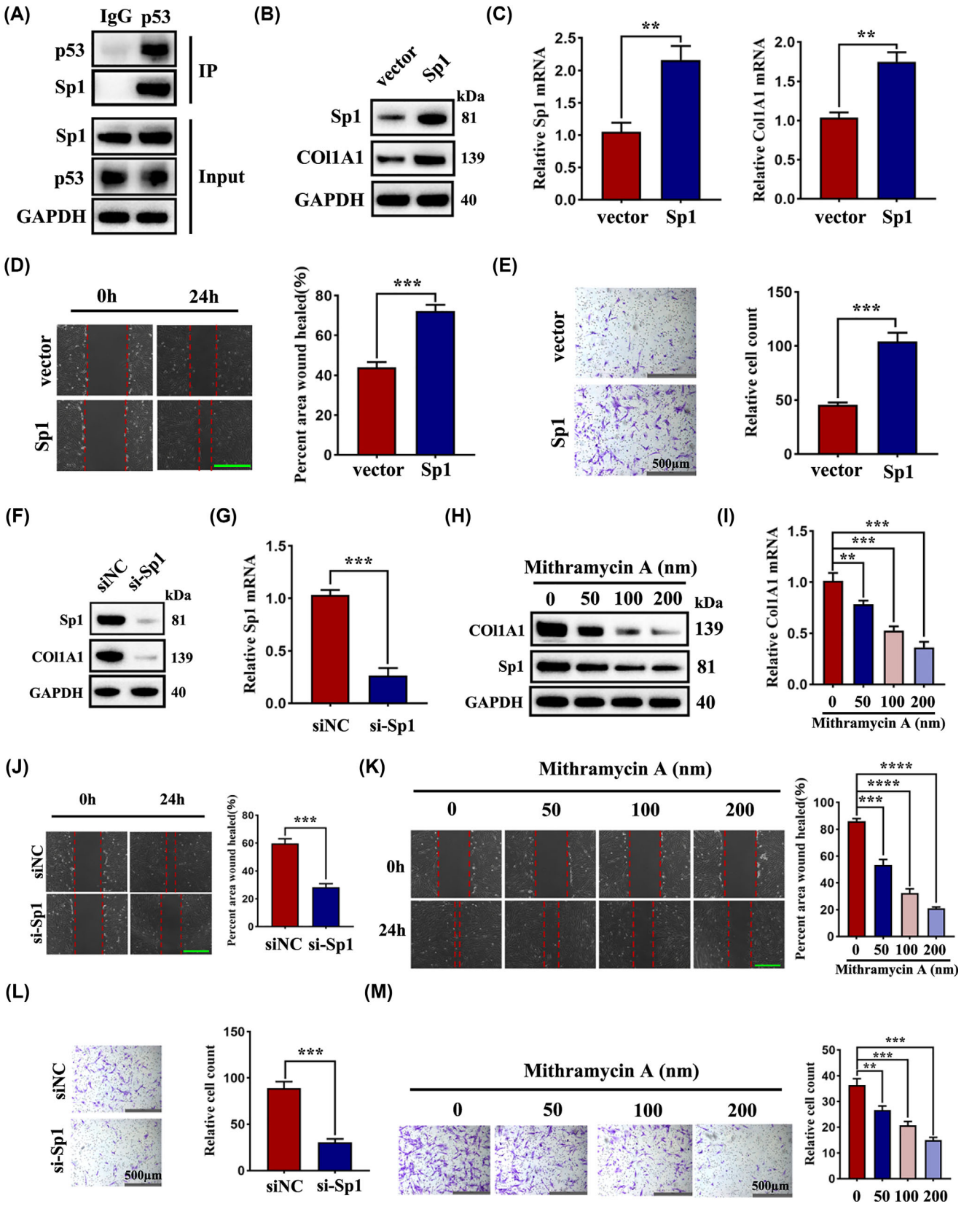

Figure 3. Sp1 promotes the expression of COL1A1 and cell migration. (**A**) Immunoprecipitation experiments validated the interaction of Sp1 and p53 in MFs. (**B**–**E**) HTFs were infected with lentiviruses expressing either Sp1 or empty control vector. Sp1 and COL1A1 expression in the indicated cells was detected by western blotting (**B**) and qPCR (**C**). The Sp1-overexpressing HTFs were subjected to wound healing (**D**) and Transwell assays (**E**). (**F**–**M**) MFs were treated with Sp1 siRNA or siNC and mithramycin A (0, 50, 100, or 200 nM). Western blotting →

←

(**F**, **H**) and qPCR (**G**, **I**) were used to detect the expression levels of Sp1 and COL1AL in indicated cells. The migration activity of the indicated cells was measured by wound healing (**J**, **K**) and Transwell assays (**L**, **M**). Data with *error bars* represent mean ± SD. $^{**}P < 0.01$, $^{***}P < 0.001$, $^{****}P < 0.0001$.

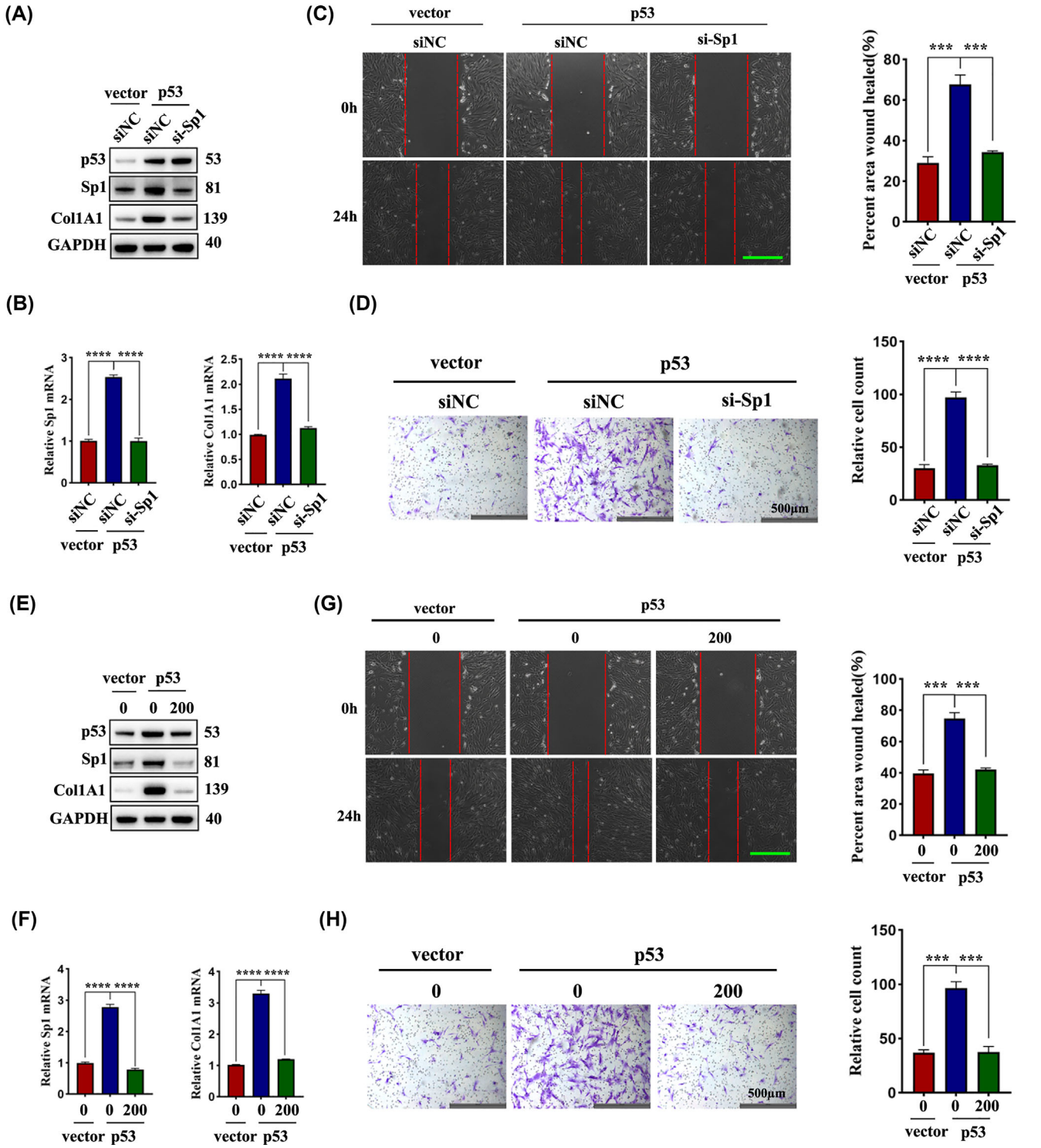

Figure 4. p53 promotes the expression of COL1A1 and cell migration via Sp1 in HTFs. (**A**–**H**) HTFs with stable p53 overexpression were treated with Sp1 siRNA or siNC and mithramycin A (0 or 200 nM). p53, Sp1, and COL1A1 protein levels were measured by western blotting (**A**, **E**). qPCR was used to evaluate the mRNA level of Sp1 and COL1A1 (**B**, **F**). The indicated cells were subjected to wound healing (**C**, **G**) and Transwell assays (**D**, **H**). Data with *error bars* represent mean ± SD. $^{***}P < 0.001$, $^{****}P < 0.0001$.

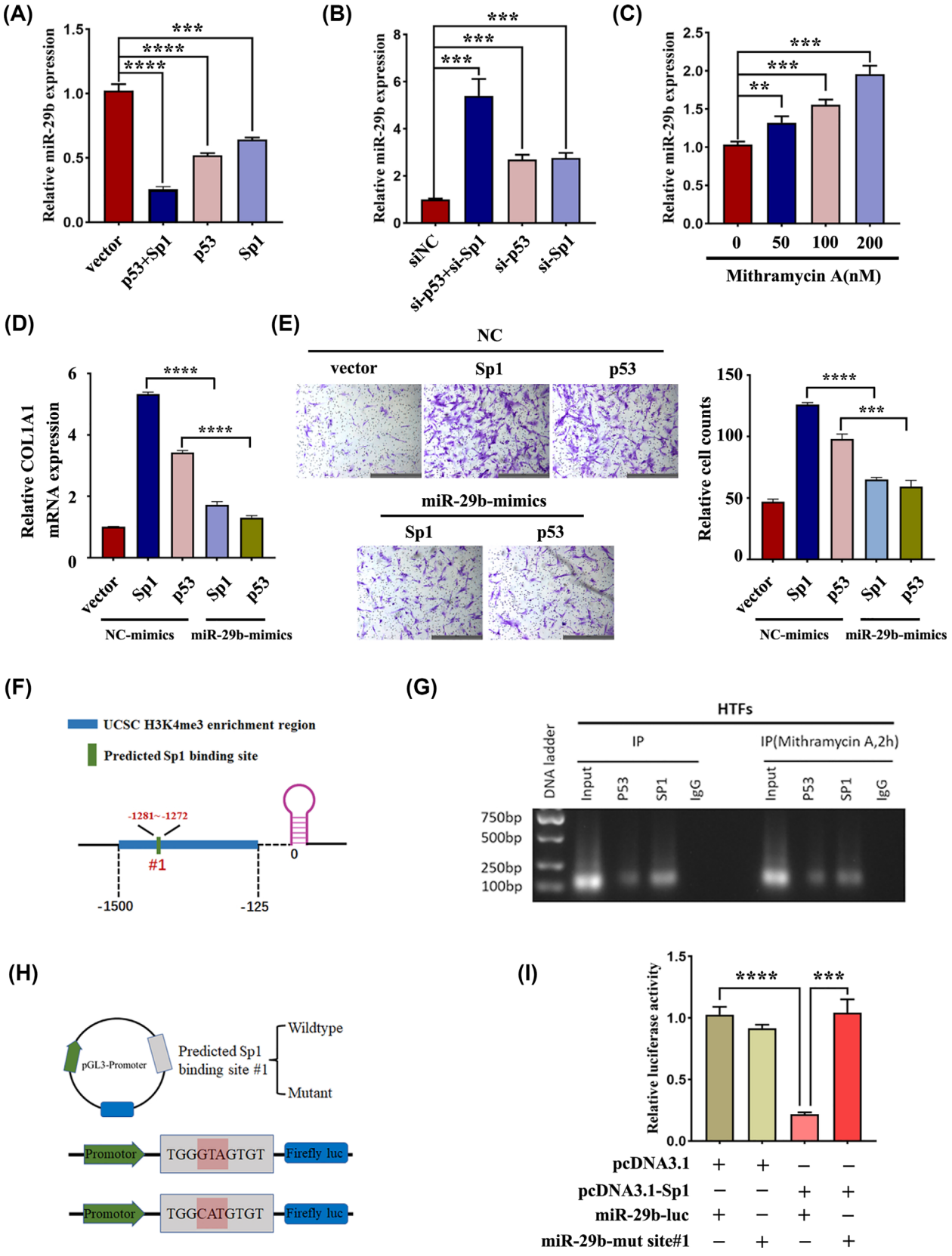

Figure 5. Sp1 binds to miR-29b promoter sites. (**A**) HTFs were infected with lentiviruses expressing either Sp1 or p53, or both. (**B**) MFs were transduced with Sp1 siRNA or p53 siRNA, or both. (**C**) MFs were treated with mithramycin A (0, 50, 100, or 200 nM). (C) MiR-29b expression was assessed by qPCR. (**D**, **E**) HTFs with Sp1 or p53 overexpression were transfected with the miR-29b mimics or negative control (NC) mimics. (**D**) qPCR was used to evaluated the mRNA level of COL1A1. (**E**) The migration ability of the indicated cells was measured by Transwell assays. (**E**) Schematic diagram of the coordinates of the miR-29b promoter region in the genome. (**G**) ChIP-PCR detected the enrichment of Sp1 and →

←

p53 in the promoter region of miR-29b. (**H**) Graphical explanation for construction of luciferase reporters. The wild-type or mutant sequence of the Sp1 binding site was inserted into a pGL3 promoter plasmid between the firefly and *Renilla* elements. (**I**) The recombinant reporter plasmid was cotransfected into HEK-293T cells with pcDNA3.1-Sp1 or an empty vector (pcDNA3.1). The indicated cells were subjected to detection of luciferase activity. Data with *error bars* represent mean ± SD. $^{**}P < 0.01$, $^{***}P < 0.001$, $^{****}P < 0.0001$.

Next, we further determined whether Sp1 binds to the miR-29b promoter region to inhibit its expression. Studies have shown that H3K4me3 histone modifications are highly abundant at promoter regions.[29] Therefore, we first searched the University of California, Santa Cruz (UCSC) genome browser (http://genoime.ucsc.edu/) to identify H3K4me3 histone modification positions upstream of the miR-29b gene. The results showed that a genomic region located approximately 1,251,500 bp upstream of the miR-29b stem-loop was enriched for H3K4me3 histone modifications (Fig. 5F). Subsequently, a potential Sp1 binding site (site 1; −1272/−1281, TGGGTAGTGT) was identified in this region by using the JASPAR database (http://jaspar.genereg.net/) (Fig. 5F). ChIP assays were performed to investigate whether Sp1 could bind to this site. As predicted, Sp1 bound the miR-29b promoter at site 1, and there was reduced enrichment upon mithramycin A treatment, indicating that this site may have an important role in the transcription of miR-29b (Fig. 5G). Furthermore, we generated a miR-29b promoter luciferase reporter containing a region around site 1 (Fig. 5H) The recombinant reporter plasmid was then cotransfected into HEK-293T cells with pcDNA3.1-Sp1 or an empty vector (pcDNA3.1). Sp1 overexpression significantly reduced the luciferase activity, whereas the attenuated transcriptional activity was reversed when the potential Sp1 binding site was mutated, suggesting that Sp1 plays an inhibitory role in miR-29b transcription (Fig. 5I). Taken together, these results show that Sp1 can bind to the miR-29b promoter region to inhibit its expression.

Treatment With Mithramycin a Suppresses Pathological Scarring In Vivo

Next, we performed GFS on adult male New Zealand White rabbits with chronic ocular hypertension (Fig. 6A). We conducted daily examinations to identify any changes at the surgical site and to assess bleb vascularity. According to the Wuerzburg bleb classification system (WBCS) scores,[30] there was a significant difference between the experimental and control groups ($P < 0.05$) (Figs. 6B, 6C). There were also significant differences among the four operation groups ($P < 0.05$) on postoperative day 28 (Figs. 6D–6F). After 28 days, we performed Masson's trichrome staining to detect the proliferation and distribution of fibrous connective tissue. The result indicated that mithramycin A treatment inhibited scarring formation after GFS, and we found that mithramycin A treatment resulted in a marked increase in miR-29b level and in a dramatic reduction in COL1A1 expression. Taken together, inhibition of the p53/Sp1/miR-29b signaling pathway by mithramycin A treatment strongly reduced pathological scarring in the experimental rabbits.

Discussion

After more than 40 years of development, trabeculectomy and implantation of aqueous humor drainage devices in glaucoma filtering surgery are considered the mainstream surgical methods for treating primary glaucoma and refractory glaucoma.[31] However, the activation of fibroblasts into myofibroblasts after surgery leads to scar formation and is the most common cause of surgical failure.[32] 5-Fluorouracil (5-FU) and mitomycin C have been widely used as antimetabolite drugs in GFS for a long time, mainly due to their inhibition of the proliferation of fibroblasts, resulting in anti-scarring effects. However, due to their poor specificity for metabolic targets, 5-FU and mitomycin C can cause certain complications, such as bleb leakage, hypotony, intraocular inflammation, and hypotonic maculopathy.[33] Moreover, although mitomycin C is available in mainland China, its price is extremely high. Currently, despite the use of minimally invasive glaucoma surgeries, GFS is still recognized as an effective treatment for glaucoma and is the preferred surgical method for treating this disease. Therefore, the development of new anti-scarring drugs that are potent and long lasting and have fewer side effects is of great significance.

In previous in vitro and in vivo studies, we observed a significant decrease in the expression level of miR-29b in filter scar tissue after GFS, and the overexpression of miR-29b can efficiently prevent the scarring of subconjunctival tissue in a preclinical model.[13,23] However, the reason for the decreased expression of miR-29b in postoperative scar is still unknown. In the present study, we determined that p53 is significantly upregulated in bleb scar tissue after GFS.

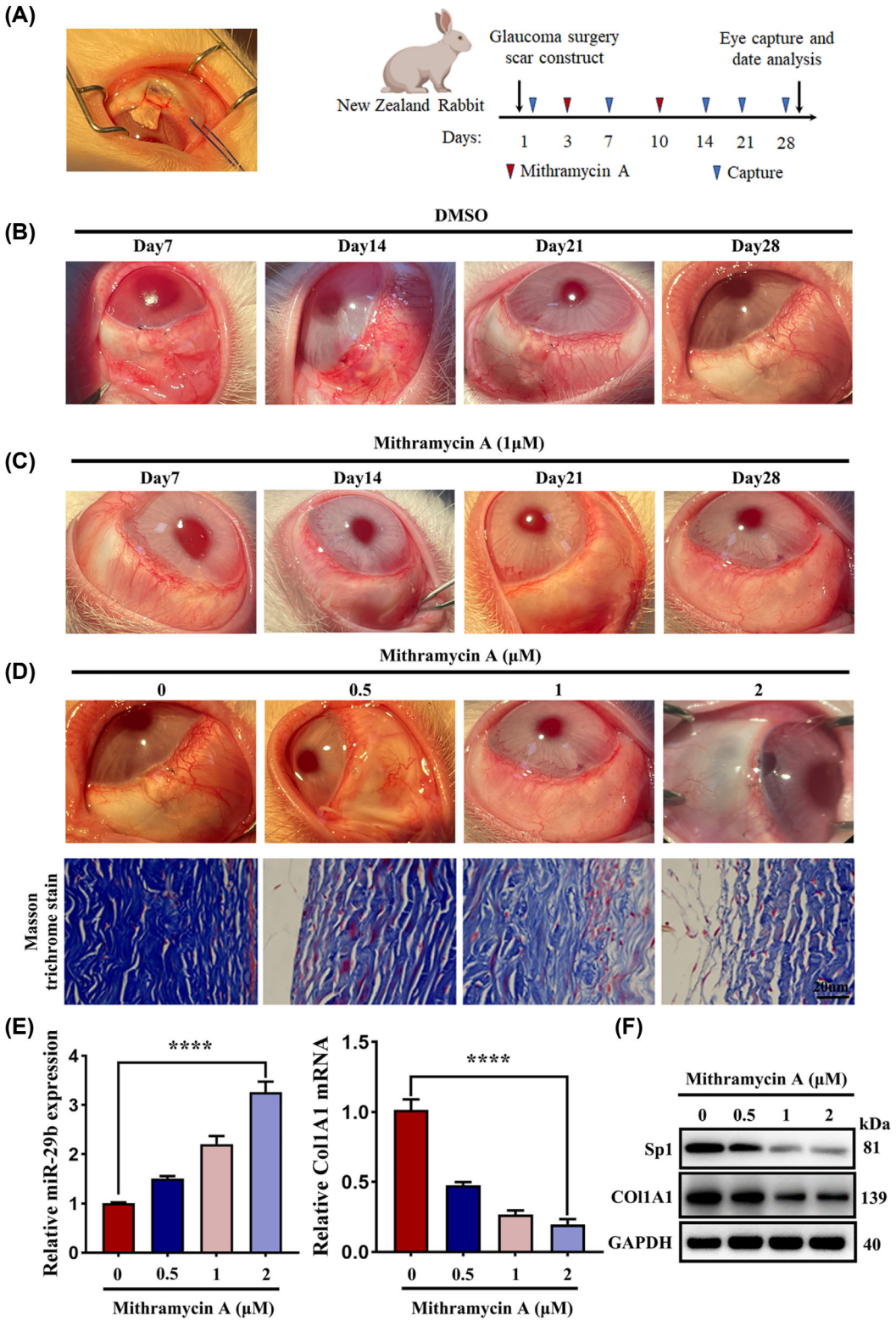

Figure 6. Treatment with mithramycin A suppresses pathological scarring in rabbit trabeculectomy models. (**A**) Graphical explanation for construction of GFS experimental model (*right panel*) and the surgical incision on the eye of the rabbit (*left panel*). (**B**, **C**) Surgical areas were treated with a subconjunctival injection of 1-μM mithramycin A or DMSO. Photographs of rabbits' eyes confirmed the filtering bleb condition at postoperative 4 weeks. Panel B is the control group, and panel C is the rabbit trabeculectomy group. (**D**–**F**) Surgical areas were treated with a subconjunctival injection with different concentrations of mithramycin A (0, 0.5, 1, or 2 μM). At the end of the experiment (postoperative day 28), the eye of the rabbit was enucleated for Masson's trichrome staining. (**D**) Photographs of filtering blebs (*upper panel*); Masson's →

←

trichrome staining (*lower panel*). *Scale bar*: 20 µm. Filtered bleb tissues were subjected to qPCR (**E**) and western blotting (**F**). Data with *error bars* represent mean ± SD. ****$P < 0.0001$.

Furthermore, we found that p53 promotes the expression of COL1A1, which could promote hypertrophic scar formation and the migration of HTFs through interaction with Sp1. Given that miR-29b has been previously reported to be a suppressor of COL1A1, it is of great interest to investigate whether the p53/Sp1 pathway upregulates COL1A1 through suppression of miR-29b. Indeed, we demonstrated that the p53/Sp1 axis inhibits the expression of miR-29b through direct binding with its promoter. We also developed a rabbit model of GFS and showed that treatment with the Sp1-specific inhibitor mithramycin A suppresses pathological scarring in vivo.

p53 is widely known as a transcription factor that regulates cell physiological functions; however, the function and mechanism of p53 in bleb scarring remain controversial. Liu and colleagues[34] found that p53 can promote scar formation by facilitating the expression and secretion of extracellular matrix (ECM) proteins in cardiomyopathy. Additionally, homeobox A5 (HOXA5) counteracts the function of pathological scar-derived fibroblasts by partially activating p53 signaling.[35] However, in this study, we found an increased expression of p53 in bleb scarring. Further research has found that overexpression of p53 can promote the expression of COL1A1 and the migration of HTFs, indicating that p53 has the effect of promoting scar formation of the filter passage after GFS. In line with our results, Ladin et al.[36] reported that p53 expression was significantly higher in keloids and hypertrophic scars than in normal skin, indicating that p53 may play different roles in the various types of scar tissues with various sources. Research has shown that Sp1 can recruit other transcription factors that participate in transcriptional regulation of the target gene through binding with its promoter region.[37] For example, Kiryu-Seo et al.[38] found that damage-induced neuronal endopeptidase (DINE) is regulated by Sp1, which is associated with ATF3, c-Jun, and STAT3 in the formation of functional complexes in damaged neurons. Dabrowska et al.[39] demonstrated that nuclear factor erythroid 2–related factor 2 (Nrf2) formed a complex with Sp1 to modulate the expression of glutamine transporter SN1 in ammonia-treated astrocytes. In the present study, we demonstrated that Sp1 interacted with p53 to form a protein complex that led to significant downregulation of miR-29b in HTFs and MFs. The luciferase reporter gene assays and ChIP assays that were performed further confirmed this

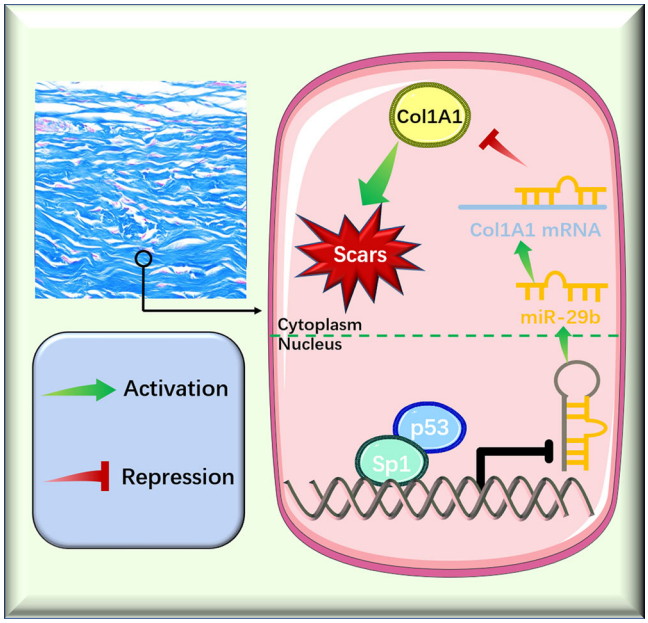

Figure 7. Schematic representation of the steps involved in p53/Sp1/miR-29b signaling regulation of scar formation in HTFs cells.

association by determining that the p53/Sp1 complex could directly bind to the promoter of miR-29b and then suppress its transcription. In line with our studies, Lin et al.[40] showed that Sp1 can bind with p53 to form complexes in the promoter region of the DNA methyltransferase 1 (DNMT1) gene, leading to an inhibition of its expression. In addition, a previous study from Schavinsky-Khrapunsky et al.[41] suggested that the formation of an Sp1-p53 heterocomplex stimulates p21 expression in Jurkat cells. Therefore, the p53/Sp1 complex plays a critical role in regulation of gene expression.

This study has some limitations. To the best of our knowledge, previous studies have acknowledged five contributions to ECM development and loss of porosity in GFS. In this study, we discovered that the p53/Sp1/miR-29b pathway may increase the expression of COL1A1, thereby accelerating HTF activation and MF conversion. In the future, we would like to investigate whether the five contributions to ECM development influence scar formation after GFS, at least partially, through the p53/Sp1/miR-29b pathway.

In summary, we demonstrated that elevated p53 levels are an important factor in bleb scarring formation. The formation of a complex with Sp1 in the miR-29b promoter region inhibits its expression, thereby

promoting the expression of COL1A1 and accelerating the progression of bleb scarring (Fig. 7). This process can be alleviated by treatment with the Sp1 inhibitor mithramycin A. Our findings suggest that the inhibition of p53/Sp1 signaling may be a therapeutic strategy to attenuate the accumulation of collagen and prevent bleb scarring following GFS.

Acknowledgments

Supported by grants from the National Natural Science Foundation of China (81500716, 81670859, 81970801); Anhui Natural Science Foundation (2208085MH229); Natural Science Foundation of Hunan Province, China (2023JJ70014, 2019JJ4000); Projects of Research and Development in Key Areas of Hunan Province (020SK213); and Research Fund of Anhui Medical University (2021xkj136). Also supported by The First Affiliated Hospital of Anhui Medical University Youth Fund Cultivating Project (2020kj12); doctoral research funds of the First Affiliated Hospital of Anhui Medical University (BSKY2019039); and Scientific Research Projects of Colleges and Universities in Anhui Province (2022AH051176).

Disclosure: **N. Li**, None; **Z. Wang**, None; **F. Yang**, None; **W. Hu**, None; **X. Zha**, None; **X. Duan**, None

* NL and ZW contributed equally to this work.

References

1. Mohan N, Chakrabarti A, Nazm N, Mehta R, Edward DP. Newer advances in medical management of glaucoma. *Indian J Ophthalmol*. 2022;70(6):1920–1930.
2. Tham YC, Li X, Wong TY, Quigley HA, Aung T, Cheng CY. Global prevalence of glaucoma and projections of glaucoma burden through 2040: a systematic review and meta-analysis. *Ophthalmology*. 2014;121(11):2081–2090.
3. de Oliveira CM, Ferreira JLM. Overview of cicatricial modulators in glaucoma fistulizing surgery. *Int Ophthalmol*. 2020;40(10):2789–2796.
4. Gater R, Ipek T, Sadiq S, et al. Investigation of conjunctival fibrosis response using a 3D glaucoma Tenon's capsule + conjunctival model. *Invest Ophthalmol Vis Sci*. 2019;60(2):605–614.
5. Acott TS, Vranka JA, Keller KE, Raghunathan V, Kelley MJ. Normal and glaucomatous outflow regulation. *Prog Retin Eye Res*. 2021;82:100897.
6. Shu DY, Lovicu FJ. Myofibroblast transdifferentiation: the dark force in ocular wound healing and fibrosis. *Prog Retin Eye Res*. 2017;60:44–65.
7. Cheng WS, Chen CL, Chen JT, et al. AR12286 alleviates TGF-β-related myofibroblast transdifferentiation and reduces fibrosis after glaucoma filtration surgery. *Molecules*. 2020;25(19):4422.
8. Diener C, Keller A, Meese E. Emerging concepts of miRNA therapeutics: from cells to clinic. *Trends Genet*. 2022;38(6):613–626.
9. Chung YW, Bae HS, Song JY, et al. Detection of microRNA as novel biomarkers of epithelial ovarian cancer from the serum of ovarian cancer patients. *Int J Gynecol Cancer*. 2013;23(4):673–679.
10. Lee JW, Guan W, Han S, Hong DK, Kim LS, Kim H. MicroRNA-708-3p mediates metastasis and chemoresistance through inhibition of epithelial-to-mesenchymal transition in breast cancer. *Cancer Sci*. 2018;109(5):1404–1413.
11. Zhong L, Zheng C, Fang H, Xu M, Chen B, Li C. MicroRNA-1270 is associated with poor prognosis and its inhibition yielded anticancer mechanisms in human osteosarcoma. *IUBMB Life*. 2018;70(7):625–632.
12. Wang WH, Deng AJ, He SG. A key role of microRNA-26a in the scar formation after glaucoma filtration surgery. *Artif Cells Nanomed Biotechnol*. 2018;46(4):831–837.
13. Li N, Cui J, Duan X, Chen H, Fan F. Suppression of type I collagen expression by miR-29b via PI3K, Akt, and Sp1 pathway in human Tenon's fibroblasts. *Invest Ophthalmol Vis Sci*. 2012;53(3):1670–1678.
14. McKinley KL, Cheeseman IM. Large-scale analysis of CRISPR/Cas9 cell-cycle knockouts reveals the diversity of p53-dependent responses to cell-cycle defects. *Dev Cell*. 2017;40(4):405–420.e2.
15. Hu J, Cao J, Topatana W, et al. Targeting mutant p53 for cancer therapy: direct and indirect strategies. *J Hematol Oncol*. 2021;14(1):157.
16. Peng T, Liu M, Hu L, et al. LncRNA Airn alleviates diabetic cardiac fibrosis by inhibiting activation of cardiac fibroblasts via a m6A-IMP2-p53 axis. *Biol Direct*. 2022;17(1):32.
17. Liu Y, Bi X, Xiong J, et al. MicroRNA-34a promotes renal fibrosis by downregulation of Klotho in tubular epithelial cells. *Mol Ther*. 2019;27(5):1051–1065.
18. Liu G, Wei C, Yuan S, et al. Wogonoside attenuates liver fibrosis by triggering hepatic stellate cell fer-

roptosis through SOCS1/P53/SLC7A11 pathway. *Phytother Res*. 2022;36(11):4230–4243.
19. Song L, Chen TY, Zhao XJ, et al. Pterostilbene prevents hepatocyte epithelial-mesenchymal transition in fructose-induced liver fibrosis through suppressing miR-34a/Sirt1/p53 and TGF-β1/Smads signalling. *Br J Pharmacol*. 2019;176(11):1619–1634.
20. Jing Y, Jian-Xiong Y. Human tissue factor pathway inhibitor-2 suppresses the wound-healing activities of human Tenon's capsule fibroblasts in vitro. *Mol Vis*. 2009;15:2306–2312.
21. Li H, Liu P, Li D, et al. STAT3/miR-130b-3p/MBNL1 feedback loop regulated by mTORC1 signaling promotes angiogenesis and tumor growth. *J Exp Clin Cancer Res*. 2022;41(1):297.
22. Wan X, Zhou M, Huang F, et al. AKT1-CREB stimulation of PDGFRα expression is pivotal for PTEN deficient tumor development. *Cell Death Dis*. 2021;12(2):172.
23. Yu J, Luo H, Li N, Duan X. Suppression of type I collagen expression by miR-29b via PI3K, Akt, and Sp1 pathway, part II: an in vivo investigation. *Invest Ophthalmol Vis Sci*. 2015;56(10):6019–6028.
24. Ortuño MJ, Susperregui AR, Artigas N, Rosa JL, Ventura F. Osterix induces Col1a1 gene expression through binding to Sp1 sites in the bone enhancer and proximal promoter regions. *Bone*. 2013;52(2):548–556.
25. Oppenheim A, Lahav G. The puzzling interplay between p53 and Sp1. *Aging (Albany NY)*. 2017;9(5):1355–1356.
26. Li H, Zhang Y, Ströse A, Tedesco D, Gurova K, Selivanova G. Integrated high-throughput analysis identifies Sp1 as a crucial determinant of p53-mediated apoptosis. *Cell Death Differ*. 2014;21(9):1493–1502.
27. Blume SW, Snyder RC, Ray R, Thomas S, Koller CA, Miller DM. Mithramycin inhibits SP1 binding and selectively inhibits transcriptional activity of the dihydrofolate reductase gene in vitro and in vivo. *J Clin Invest*. 1991;88(5):1613–1621.
28. Vizcaíno C, Mansilla S, Portugal J. Sp1 transcription factor: a long-standing target in cancer chemotherapy. *Pharmacol Ther*. 2015;152:111–124.
29. Schneider R, Bannister AJ, Myers FA, Thorne AW, Crane-Robinson C, Kouzarides T. Histone H3 lysine 4 methylation patterns in higher eukaryotic genes. *Nat Cell Biol*. 2004;6(1):73–77.
30. Furrer S, Menke MN, Funk J, Toteberg-Harms M. Evaluation of filtering blebs using the 'Wuerzburg bleb classification score' compared to clinical findings. *BMC Ophthalmol*. 2012;12:24.
31. Razeghinejad MR, Spaeth GL. A history of the surgical management of glaucoma. *Optom Vis Sci*. 2011;88(1):E39–E47.
32. Hollo G. Wound healing and glaucoma surgery: modulating the scarring process with conventional antimetabolites and new molecules. *Dev Ophthalmol*. 2017;59:80–89.
33. Halili A, Kessel L, Subhi Y, Bach-Holm D. Needling after trabeculectomy – does augmentation by anti-metabolites provide better outcomes and is mitomycin C better than 5-fluoruracil? A systematic review with network meta-analyses. *Acta Ophthalmol*. 2020;98(7):643–653.
34. Liu X, Burke RM, Lighthouse JK, et al. p53 Regulates the extent of fibroblast proliferation and fibrosis in left ventricle pressure overload. *Circ Res*. 2023;133(3):271–287.
35. Liang Y, Zhou R, Fu X, Wang C, Wang D. HOXA5 counteracts the function of pathological scar-derived fibroblasts by partially activating p53 signaling. *Cell Death Dis*. 2021;12(1):40.
36. Ladin DA, Hou Z, Patel D, et al. p53 and apoptosis alterations in keloids and keloid fibroblasts. *Wound Repair Regen*. 1998;6(1):28–37.
37. Samson SL, Wong NC. Role of Sp1 in insulin regulation of gene expression. *J Mol Endocrinol*. 2002;29(3):265–279.
38. Kiryu-Seo S, Kato R, Ogawa T, Nakagomi S, Nagata K, Kiyama H. Neuronal injury-inducible gene is synergistically regulated by ATF3, c-Jun, and STAT3 through the interaction with Sp1 in damaged neurons. *J Biol Chem*. 2008;283(11):6988–6996.
39. Dabrowska K, Skowronska K, Popek M, Albrecht J, Zielinska M. The role of Nrf2 transcription factor and Sp1-Nrf2 protein complex in glutamine transporter SN1 regulation in mouse cortical astrocytes exposed to ammonia. *Int J Mol Sci*. 2021;22(20):11233.
40. Lin RK, Wu CY, Chang JW, et al. Dysregulation of p53/Sp1 control leads to DNA methyltransferase-1 overexpression in lung cancer. *Cancer Res*. 2010;70(14):5807–5817.
41. Schavinsky-Khrapunsky Y, Huleihel M, Aboud M, Torgeman A. Role of protein kinase C and the Sp1-p53 complex in activation of $p21^{WAF-1}$ expression by 12-*O*-tetradecanoylphorbol-13-acetate in human T cells. *Oncogene*. 2003;22(34):5315–5324.